Vulnerability of the Cordilleran Ice Sheet to iceberg calving during late Quaternary rapid climate change events

I. L. Hendy[1] and T. Cosma[1]

Received 6 February 2008; accepted 19 March 2008; published 22 May 2008.

[1] We present the first high-resolution record of iceberg calving on the continental slope of Vancouver Island, British Columbia (MD02-2496, 48°58N, 127°02W, 1243 m water depth), through the last glacial from the Cordilleran Ice Sheet (CIS). These previously unknown ice-rafted debris (IRD) events representing significant retreat of the western margin of the CIS out of marine waters show little correspondence with local climate change. High-resolution radiocarbon dating indicates that the younger IRD events coincide with global radiocarbon age plateaus that allow direct correlation with distal climate records where the same plateaus have been identified. The coincidence of episodic shedding of IRD from the CIS with North Atlantic climate events (i.e., North Atlantic Deep Water shutdown, and Heinrich events) begs the question: What drove CIS destabilization? Forcing appears to be external to CIS dynamics perhaps resulting from either eustatic sea level rise or episodes of atmospheric warming over the North American continent.

Citation: Hendy, I. L., and T. Cosma (2008), Vulnerability of the Cordilleran Ice Sheet to iceberg calving during late Quaternary rapid climate change events, *Paleoceanography*, *23*, PA2101, doi:10.1029/2008PA001606.

1. Introduction

[2] High-resolution grain size analyses of continental slope deposits off western Vancouver Island (Core MD02-2496, 48°58′47″N, 127°02′14″W, 1243 m water depth, see Figure 1) demonstrate three intervals of ice-rafted debris (IRD) deposition occurred during the last glacial interval (younger than 50 ka). Furthermore, high-resolution stable isotope results generated from analysis of planktonic foraminifera *Neogloboquadrina pachyderma* provide a continuous climate record in the core that can be directly compared to these IRD events. We demonstrate that IRD events in the region are related to ice sheet retreat in the Pacific Northwest and occur during well known North Atlantic climate events (i.e., H5, H1 and the Oldest Dryas). We suggest this apparent ice sheet destabilization supports the concept that even ice sheets distal to climatic hot spots are vulnerable to climate change.

[3] The Cordilleran Ice Sheet (CIS) initially grew in the north (Alaska) but spread south during the last glaciation reaching its maximum extent (~4000 km wide) in southern British Columbia and northern Washington. Glacial advance (the Fraser Glaciation) in southern British Columbia began around 30 ka (25 ^{14}C ka B.P., Figure 2d) [*Booth et al.*, 2004]. During this interval, ice from the Canadian Coast Mountains advanced into the Georgia Strait dividing the western ice sheet into two lobes around the Olympic Mountains, the westward flowing Juan de Fuca Lobe and the southward flowing Puget Lobe (Figure 1). When the CIS reached its maximum extent by 17.5 ka (14.5 ^{14}C ka B.P.) in Washington [*Booth et al.*, 2004; *Clague and James*, 2002; *Porter and Swanson*, 1998], it remained much smaller than the Laurentide Ice Sheet (LIS). Ice advanced onto the continental shelf near MD02-2496 (~35 km to the east at Tofino) after 19.8 ka (16.7 ^{14}C ka B.P., Figures 1 and 2d [*Blaise et al.*, 1990]).

2. Methods

[4] Samples for grain size and stable isotopic analysis were taken in 2 cm slices at a sampling resolution of 5 cm from 0 to 2400 cm below seafloor (bsf) and 3200 to 3835 cm bsf (uncorrected), and 4 cm between 2400 and 3200 cm bsf (uncorrected). Samples were washed through a 63 μm sieve using deionized water, the fine fraction (<63 μm) was collected for subsequent Coulter Counter grain size analyses, and the coarse fraction (>63 μm) was dried and weighed. Clastic grains greater than 250 μm diameter were counted and normalized to dry sample weight. Carbonate, as well as Fe and Mn oxides/hydroxides were removed from the fine fraction (<63 μm) following standard procedures [*Rea and Janecek*, 1981] before analyzing the 2 to 60 μm grain size using a Beckman Coulter Multisizer 3. The 2 to 4 μm results were extracted from the 256 bins between 2 and 60 μm reported by the Coulter Multisizer and normalized to the total sample dry weight and percent lithogenic sediment component.

[5] The location of MD02-2496 on the continental slope of Vancouver Island potentially allows for the transportation of fine sand particles by processes other than ice rafting. Although the temporal distribution of >125 and >250 μm grains within the record is similar, >250 μm grains are less frequent. There are no grains >250 μm in ~51% of MD02-2496 samples. Therefore within MD02-2496, we employ a less common definition of

[1]Department of Geological Sciences, University of Michigan, Ann Arbor, Michigan, USA.

0883-8305/08/2008PA001606

IRD as number of grains >250 μm grains g^{-1} [*Bischof and Darby*, 1997; *Blaise et al.*, 1990; *St John and Krissek*, 1999]. Furthermore no graded sedimentary features were observed in association with the IRD events (>250 μm grains g^{-1}), except at 1427 and 1457 cm bsf, respectively. These samples were subsequently removed from the database because of their possible association with downslope processes.

[6] Five to 20 specimens of the planktonic foraminifera *Neogloboquadrina pachyderma* (sinistral and dextral) from the >125 μm fraction were collected per sample and prepared using standard methods. 673 (+44 replicate) mixed sinistral and dextral *N. pachyderma,* 35 exclusively dextral and 36 sinistral *N. pachyderma* stable isotope analyses were completed using a Kiel device connected directly to a Finnigan MAT 251 mass spectrometer. Results were averaged where multiple analyses were available for a sample. O^{17} data were corrected for acid fractionation and source mixing by calibration to a best fit regression line defined by NBS-19. Machine precision was less than 0.1‰. Data are reported in standard notation relative to the Vienna Peedee belemnite (VPDB) standard.

3. Age Model

[7] Radiocarbon dating was preformed on both carbonate and organic carbon. Details of the generated age model are described by *Cosma et al.* [2008]. From the 46 ^{14}C dates generated in this study, 14 dates were averaged, and 15 dates (including, dates within radiocarbon plateaus, mixed benthic and finite age samples) were excluded from the age model. The remaining dates were used to generate 24 calibrated calendar year ages (including 6 that represent average dates, Figure 3). Calibrated calendar year ages were obtained using the full probability method of calendar age calibration [*Telford et al.*, 2004]. Reservoir-corrected ^{14}C dates younger than 22 ^{14}C ka B.P. were calibrated using CALIB04 (M. Stuiver et al., CALIB 4.0, 2004, available at www.calib) and the ^{14}C calibration data set MARINE04 [*Hughen et al.*, 2004b]. The ^{14}C ages greater than 22 ^{14}C ka B.P. were converted to calendar ages using a linear interpolation of the calibrated data set of *Hughen et al.* [2004a]. Point to point linear interpolations were used to generate ages between 0 and 992 cm bsf, and 2847 cm bsf to core bottom. The Y intercept at 0 cm bsf is 2.25 ka, which is not unreasonable as large diameter piston coring methods often lose core top material through overpenetration. Between 992 and 2847 cm bsf a 5 point polynomial was used to generate ages. Interpolated ages are expressed as ka (thousand years before present). To facilitate correlation with terrestrial radiocarbon dates, ages that are not calibrated to calendar ka remain as ^{14}C ka B.P. (thousand years before present).

[8] The close correlation between MD02-2496 and both GISP2 [*Stuiver et al.*, 1995] and the H events [*Hemming*, 2004] is shown in Figure 2f. Although several published calibration data sets beyond 22 ^{14}C ka B.P. are available [*Bard et al.*, 1998; *Fairbanks et al.*, 2005; *Hughen et al.*, 2006; *Kitagawa and van der Plicht*, 1998], the *Hughen et al.* [2004a] calibration was chosen as the calculated dates <30 ka fall mid range within the data compiled by NOTCAL04 [*van der Plicht et al.*, 2004]. Furthermore, results from *Hughen et al.* [2004a] were stratigraphically tied to GISP2, similar to many records including North Pacific cores (i.e., ODP Hole 893A and 1017E) and North Atlantic cores associated with H events [*Hemming*, 2004]. Thus we employed the more commonly used GISP2 chronology rather than the latest calibrations. This is important when attempting to determine the stratigraphic relationship between the oldest IRD event in MD02-2496 and H5. *Hemming* [2004] correlated H5 to GISP2 with an approximate age of 45 ka, however if the Hulu Cave speleothem record correlation is employed, the age of the event would fall around 47 ka [*Wang et al.*, 2001].

4. Iceberg Calving on the Cordilleran Ice Sheet

[9] MD02-2496 demonstrates that iceberg calving was not characteristic of southwestern CIS behavior throughout most of the Fraser Glaciation despite possessing a marine margin. Grain size analysis of sediments in MD02-2496 show that IRD (>250 μm grains g^{-1}, Figure 2a) was only deposited during three discrete time intervals, two of which contain dropstones (pebble-sized material), indicating iceberg calving in the region was relatively uncommon (Figure 2a). Furthermore, no evidence exists (including MD02-2496) for calving during ice sheet growth [*Porter and Swanson*, 1998], consistent with the presence of a morainal shoal during ice advance through the straits and onto the continental shelf [*Meier and Post*, 1987]. The only other record of IRD that exists in the region was found to the north in the Hecate Strait during the interval between 18.3 and 15.3 ka (15 and 13 ^{14}C ka B.P. [*Blaise et al.*, 1990]).

[10] IRD deposition off Vancouver Island (MD02-2496) began at ~17.1 ka (~14 ^{14}C ka B.P.), dramatically increased by 16.4 ka (13.8 ^{14}C ka B.P.) and peaked at 16.2 ka (13.5 ^{14}C ka B.P.) with ~450 > 250 μm grains g^{-1} (Figure 4c). This IRD event was followed by an interval of well-sorted, very fine silt (% grains between 2 and 4 μm, glacial flour, Figure 2b) deposition that began at 15.4 ka (13 ^{14}C ka B.P., Figure 2b), and was terminated by a smaller (~100 > 250 μm grains g^{-1}) episode of IRD deposition between 14.8 and 14.6 ka (12.5 ^{14}C ka B.P., Figure 2b). Another significant IRD event occurred at ~47 ± ~5 ka (~42.3 ± 1060 ^{14}C ka B.P., Figure 2a). IRD deposition began slowly at ~48.5 ka and ended abruptly with a maximum of ~500 > 250 μm grains g^{-1} by 46.5 ka. An interval of well sorted, very fine silt deposition began at ~48 ka and ended at ~46 ka (Figure 2b). Thus the 2–4 μm and >250 μm grain size records indicate short-lived intervals of significant iceberg calving from the CIS were coincident with or followed by meltwater plumes carrying glacial flour.

[11] The retreating ice margin passed through the Juan de Fuca Strait between 17.4 and 16.2 ka (14.46–13.6 ^{14}C ka B.P. [*Dethier et al.*, 1995; *Mosher and Hewitt*, 2004]). This retreat coincides with ~17 to 16.2 ka IRD event recorded at MD02-2496 reinforcing the association of IRD with CIS retreat. It is presumed that the Puget and Juan de Fuca Lobes had retreated into a single ice mass in the northern Puget Lowland by 16.2 ka with rapid northward recession

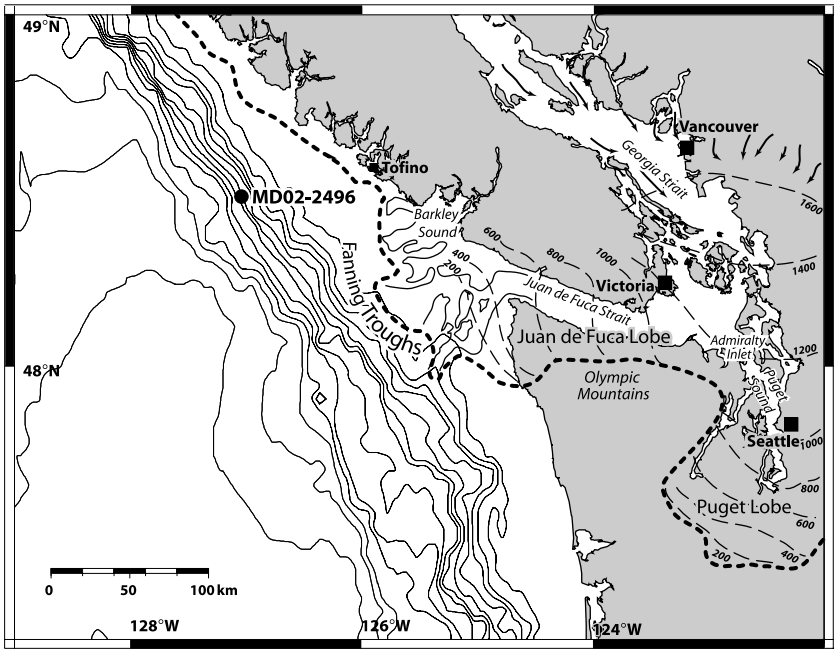

Figure 1. Location of site MD02-2496 (48°58′48″N, 127°02′14″W, 1243 m water depth) on the west coast of Vancouver Island. Heavy dashed line represents the maximum extent of the Cordilleran Ice Sheet at 15 ^{14}C ka B.P. [*Clague and James*, 2002]. Thin dashed lines represent ice sheet thickness, and arrows represent ice flow direction [*Porter and Swanson*, 1998]. Troughs outside the Juan de Fuca Strait indicate locations of grounded ice [*Herzer and Bornhold*, 1982].

via iceberg calving into the northern Puget Sound during this time [*Waitt and Thorson*, 1983]. Continued retreat of the Juan de Fuca Lobe resulted in the failure of the ice dam at Admiralty Inlet and incursion of marine waters into Puget Sound about 15.3 ka (13 ^{14}C ka B.P. [*Thorson*, 1980]), eventually beheading the Puget Lobe from its ice supply [*Waitt and Thorson*, 1983]. A calving embayment began to develop in the Strait of Georgia at 15.3 ka [*Clague and James*, 2002] and the Strait was completely deglaciated by 14.6 ka (12.5 ^{14}C ka B.P. [*Guilbault et al.*, 2003]). This calving embayment is coincident with the most recent IRD event at MD02-2496. Isostatic uplift in response to deglaciation was exceptionally fast suggesting extremely rapid wastage of ice at ~14.6 ka [*Clague and James*, 2002], reinforcing iceberg calving as an efficient export mechanism for rapid ice sheet retreat. Following these iceberg calving events, the CIS retreated onto the continent, unable to advance until conditions again become favorable for ice growth (>10,000 years).

5. Radiocarbon Plateaus

[12] Another important observation is that the two most recent IRD events occur near the termination of radiocarbon plateaus (Figure 4). Radiocarbon plateaus within sediment cores can be generated by a number of processes including, mixing with a secondary source of radiogenic carbon, instantaneous deposition of a thick package of sediment, and global changes in ^{14}C production and partitioning in carbon reservoirs. On the basis of $\delta^{13}C_{organic\ carbon}$, 50 to 70% of late glacial total organic carbon accumulation has been estimated to be terrestrial in origin [*Cosma et al.*, 2008; *McKay et al.*, 2004], potentially carrying an infinite radiocarbon age such that bulk organic carbon radiocarbon ages are <4 ka older than the planktonic foraminiferal carbonate when the CIS was proximal to the site [*Cosma et al.*, 2008]. As well the CIS might have increased ^{14}C depleted CO_2 delivery to surface waters through meltwater [*Hutchinson et al.*, 2004; *Kovanen and Easterbrook*, 2002]. Although surface water reservoir ages appear to have increased during the late glacial from 807 ± 50 years to >1,400 years [*Cosma et al.*, 2008], we reject local changes in reservoir ages as a radiocarbon plateau generating mechanism for the following reasons. First terrestrial organic carbon delivery to the site was greatest when the CIS was proximal [*Cosma et al.*, 2008] and should have been coincident with the radiocarbon plateaus if terrestrial organic carbon had significantly impacted the ^{14}C of marine pCO_2. Second the addition of ^{14}C depleted carbon to the marine environment would have a greater impact on surface waters than deep resulting in decreased benthic-planktonic foraminiferal age differences, which is inconsistent with results from a nearby sediment core [*McKay et al.*, 2005].

[13] Sediment delivery within a geologically instantaneous time interval such as might result from turbidity current may also produce an apparent radiocarbon plateau. MD02-2496 is indeed rich in sedimentary structure. Cyclic sedimentation associated with alternating sediment color, high-low magnetic susceptibility, and occasional sand layers

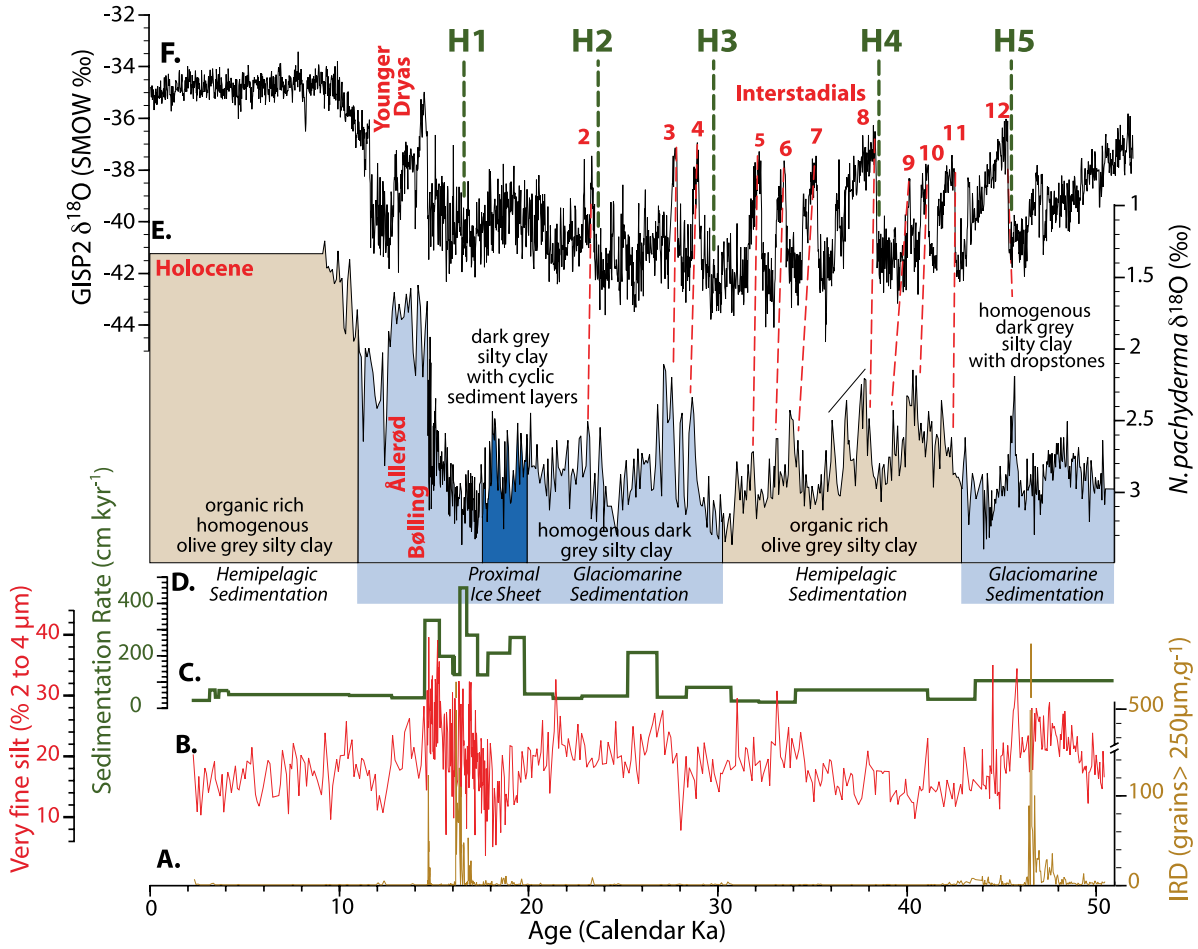

Figure 2. Comparison of climate records in the North Atlantic and North Pacific. (a) Ice-rafted debris or IRD (number of grains greater than 250 μm g^{-1}, gold). (b) Percent of terrigenous sediment between 2 and 4 μm (red). (c) Sedimentation rate (cm ka^{-1}, green), (d) Core stratigraphy. (e) *N. pachyderma* δ^{18}O (‰ Vienna Peedee belemnite (VPDB), black) against calibrated calendar years from MD02-2496, Vancouver Island. Stratigraphy key is as follows: Beige represents organic-rich, homogenous olive gray silty clay. Light blue represents homogenous dark gray silty clay. Dark blue represents dark gray silty clay with cyclic sediment layers. (f) Comparison with GISP2 from the Greenland Ice Sheet (black [*Stuiver and Grootes*, 2000]). Interstadial events correlated between the cores are identified by a dashed red line, while Heinrich events (H events [*Hemming*, 2004]) in the North Atlantic are indicated by dashed green lines. Major climate events are labeled alongside identified interstadials.

(several mm thick) occurs between 19 and 17 ka when the ice sheet was proximal. In contrast variability in color and magnetic susceptibility during the intervals containing the 13.3 and 12.2 ^{14}C ka B.P. events shows no cyclic behavior although the magnitude of variability is similar. More importantly there are no large-scale sediment structures (i.e., the normal grain size grading) indicative of instantaneous sedimentary events. We therefore argue that neither the 3 m of sediment associated with the 13.3 ^{14}C ka B.P. event, nor the ~75 cm of sediment associated with the 12.2 ^{14}C ka B.P. event were instantaneously deposited.

[14] Globally, a 13.6% or 190 ‰ decrease in the ^{14}C to C ratio occurs over the interval between Heinrich 1 (H1) and the Bølling [*Broecker and Barker*, 2007], in which the 12.2 and 13.3 ^{14}C ka B.P. radiocarbon plateaus [*Hughen et al.*, 2004a] occur. Cosmogenic nuclide concentrations were invariant during this interval indicating the plateaus did not originate from variations in ^{14}C production but instead were related to changes in the global carbon reservoir. The largest, easily exchangeable carbon reservoir is the deep ocean, and it is assumed that these plateaus were related to changes in NADW production and subsequent changes in atmosphere-ocean carbon partitioning [*Broecker and Barker*, 2007; *Hughen et al.*, 2004a]. Much evidence exists for a reduction in NADW export [*McManus et al.*, 2004] during H events as melting iceberg armadas from the LIS formed a low-density cap over the North Atlantic, preventing deep water formation [*van Kreveld et al.*, 2000] and subsequently drawdown of newly produced ^{14}C from the atmosphere. However, the release of old radiocarbon from the deep

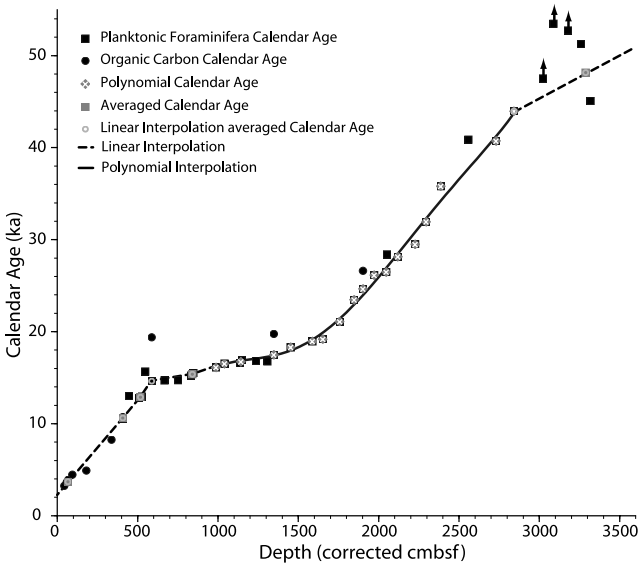

Figure 3. Age in calendar years B.P. versus core depth (corrected cm bsf). Dates were generated using planktonic foraminiferal carbonate (solid squares) and bulk organic carbon (solid circles). Ages were also generated using the average of multiple dates (shaded squares). Ages (open circles) that were used in the linear interpolation portion of the age model (dashed line) are shown with those (patterned diamonds) used in the polynomial interpolation portion of the age model. Arrows represent finite age samples.

Southern Ocean has also been implicated in the drop in atmospheric radiocarbon activity between H1 and the Bølling [*Marchitto et al.*, 2007].

[15] These radiocarbon plateaus are currently recognized in the North Atlantic [*Voelker et al.*, 1998], Cariaco Basin (Figure 4a) [*Hughen et al.*, 2004a], Santa Barbara Basin [*Sarnthein et al.*, 2007] and the North Pacific (Figure 4g) [*Sarnthein et al.*, 2006]. Carbon is rapidly mixed in the atmosphere; therefore, the plateaus should be globally geologically instantaneous and allow for independent stratigraphic correlation of widely distributed study sites [*Sarnthein et al.*, 2007]. Thus, we infer that the 13.5 ^{14}C ka B.P. IRD event is coincident with H1 and the 12.5 ^{14}C ka B.P. with the Oldest Dryas (as defined by *Hendy et al.* [2002]). From this we postulate that the oldest CIS IRD event at ~47 ka in MD02-2496 occurs at H5 as this date fits well within the error of both ^{14}C dating and calibration.

6. Triggers for Cordilleran Ice Sheet Calving

[16] Why would the iceberg calving of the southern CIS be coincident with H5, H1 and the Oldest Dryas? The timing appears related to the vulnerability of the ice sheet to climate change in the North Atlantic. The influence of H events on NADW export and/or the LIS may have orchestrated CIS behavior through such processes as atmospheric warming [*Clark et al.*, 2007] or sea level rise [*Rohling et al.*, 2004]. The existence of ice sheets with marine margins resting on beds below sea level depends on ice thickness relative to sea level [*Clarke*, 1987]. If ice thins or sea level rises, the ice sheet margin may begin to float. Troughs fanning outward away from the Juan de Fuca Strait and Barkley Sound provide evidence for grounding of the CIS on the continental shelf (Figure 1) [*Herzer and Bornhold*, 1982]. Excellent preservation of the troughs as well as the lack of glacial sediment infilling suggests extremely rapid ice withdrawal from the shelf, exceeding the rate of marine transgression [*Herzer and Bornhold*, 1982].

[17] Eustatic rises in sea level of between 6 and 15 m have been predicted during H events [*Hemming*, 2004]. However, the sea level data record during H1 is poorly constrained (Figure 4b). An estimated 12 [*Bard et al.*, 1990] to 30 m [*Siddall et al.*, 2003] rise occurred between 17 to 15 ka, while a 6 m sea level rise occurred at ~14.7 ka [*Bard et al.*, 1990]. Although North Atlantic meltwater is implicated in this sea level rise, recent studies suggest that the Antarctic contributed more to MIS 3 sea level variations than previously anticipated [*Rohling et al.*, 2004]. Sea level forcing of ice sheet retreat may require a rise exceeding >10 m based on recent observations of sediment deposition at Antarctic Ice Stream grounding lines [*Alley et al.*, 2007; *Anandakrishnan et al.*, 2007]. These show that frictional drag results in restricted flow and ice thickening over the grounding line, stabilizing it against sea level rises less than ~10 m [*Alley et al.*, 2007]. Further, if sufficient sea level rise occurs (>5 m) to allow flotation, subsequent high subglacial sediment deposition rates can increase terminal moraine height and quickly restabilize the grounding line [*Alley et al.*, 2007; *Anandakrishnan et al.*, 2007].

[18] A ~1.1 m thinning of floating ice has a similar effect on flotation as a 1 m rise in sea level [*Alley et al.*, 2007] and a 1°C air temperature warming can increase surface melt rate by >10 cm a^{-1}. Therefore, atmospheric warming could also provide a trigger for rapid ice sheet retreat. The high-resolution *N. pachyderma* δ^{18}O results from MD02-2496 provide a continuous climate record in the core that can be directly compared to intervals of ice-rafted debris (IRD). Yet, this record demonstrates no notable surface ocean warming or cooling prior to or coincident with the IRD events (Figure 4e). Perhaps melting ice locally masked surface ocean warming in the region as evidence for warming is found further afield.

[19] Ocean warming at 16.8 ka has been demonstrated in the northwest Pacific (Figure 4f) [*Sarnthein et al.*, 2006] suggesting North Pacific sea surface temperature anomalies similar to the positive phase of the Pacific/North American teleconnection pattern (PNA) [*Minobe and Mantua*, 1999] existed during this time. Similarly a ~4.5°C warming at ~16.75 ka has been found in Santa Barbara Basin [*Hill et al.*, 2006]. Cooling synchronous with the CIS IRD events in the northeast Pacific Ocean may be coincident with atmospheric warming over the North American continent. Thus regional atmospheric warming may have led to the rapid retreat of the southern portion of the CIS. This premise is supported by the coincidence (within dating error) of Puget Lobe downwasting [*Porter and Swanson*, 1998] with Glacial Lake Missoula, created by meltwater drainage

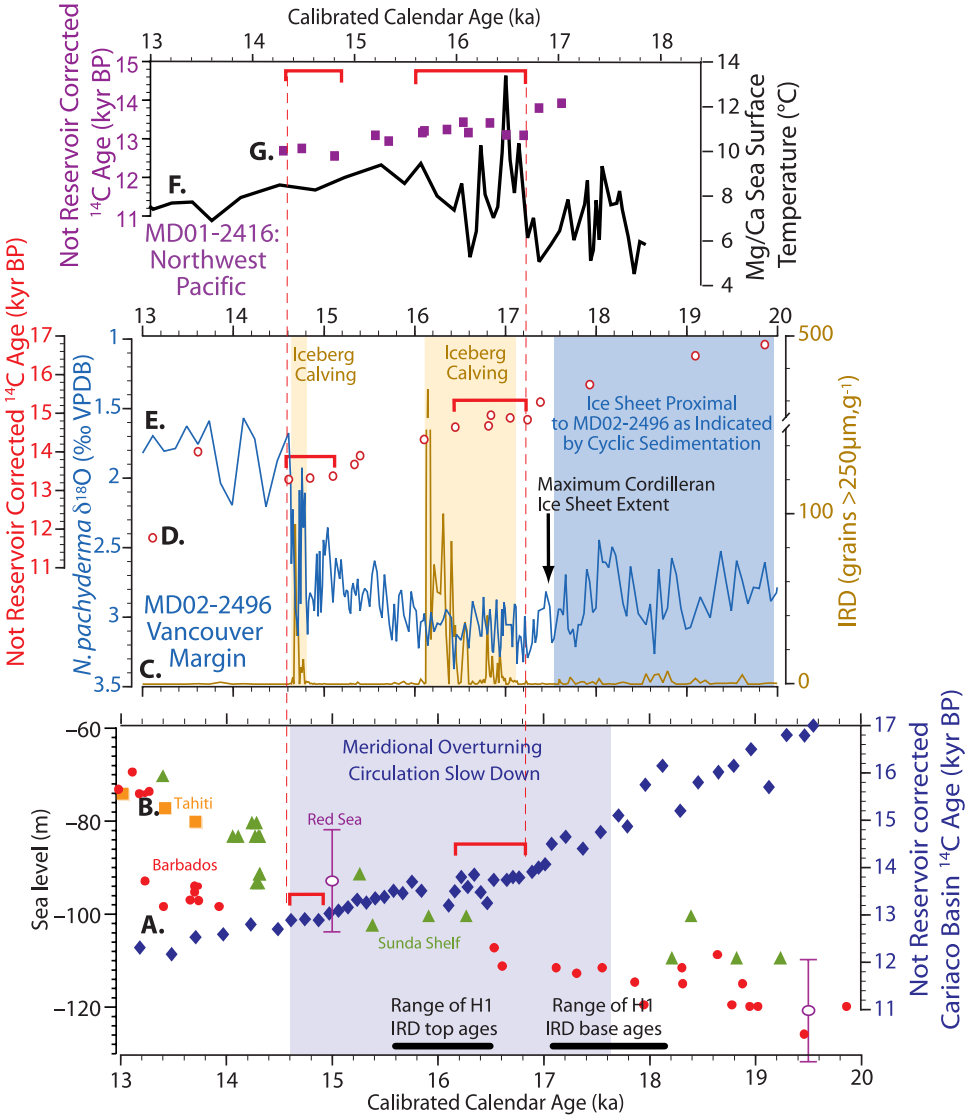

Figure 4. Time interval spanning 20 to 13 ka displays (a) ^{14}C dates not corrected for reservoir effects from ODP Cariaco Basin (dark blue diamonds [*Hughen et al.*, 2004a]) and (b) sea level data from the Red Sea (open purple circles [*Siddall et al.*, 2003]), Barbados (solid red circles [*Bard et al.*, 1990; *Fairbanks*, 1989]), and Tahiti (orange squares [*Bard et al.*, 1996]) and the Sunda Shelf (green triangles [*Haneburth et al.*, 2000]). (c) IRD (number of grains greater than 250 μm g^{-1}, gold). (d) The ^{14}C dates not corrected for reservoir effects (open red circles). (e) *N. pachyderma* δ^{18}O (‰ VPDB, blue) from MD02-2496, Vancouver Island. (f) Mg/Ca sea surface temperature (°C, black). (g) The ^{14}C dates not corrected for reservoir effects (purple squares) from MD01-2416, northwestern Pacific [*Sarnthein et al.*, 2006]. The ranges of Heinrich 1 calibrated ages within North Atlantic cores are displayed by black bars. The ^{14}C plateaus are indicated by red bars, and plateaus in each region are correlated by dashed lines.

dammed by the eastern lobes of the CIS [*Atwater*, 1986] during early deglaciation [*Clague et al.*, 2003]. Alternately thinning may also result from changes in ice sheet mass balance through climatically driven precipitation change, however, pollen records indicate that northern Washington became cooler and drier as the CIS advanced (30 to 25 ka) and wetter as the ice sheet retreated at 17 ka [*Grigg and Whitlock*, 2002].

[20] If the CIS was susceptible to detachment from grounding lines in association with rapid climate change, why then are there no IRD events coincident with H2, 3 and 4? The final aspect of the ice sheets vulnerability lies in the fact that a significant body of ice is required both to isostatically depress the Georgia Strait/Puget Lowland area and maintain a marine margin that extends onto the shelf. As there was no ice sheet present in the region during H4 [*Booth et al.*, 2004; *Clague and James*, 2002], ice occupied only the Fraser lowland area during H2 [*Clague and James*, 2002], and H3 is considered minor in comparison to other North Atlantic IRD events

[*Hemming*, 2004], we would predict no CIS response to these events. We note, however, that there is only one local study supporting the presence of an ice sheet during H5 [*Easterbrook*, 1986], while there are numerous locations in the Puget Lowland area [*Booth et al.*, 2004] and eastern British Columbia that were ice free sometime prior to ~50 ka [*Clague and James*, 2002].

[21] The rapid retreat of the CIS at H5 and H1 supports the concept of a global ice sheet destabilization process such that ice sheets that were distal to the North Atlantic and/or Antarctic were vulnerable to climate change in those regions providing a marine margin existed. Rapid retreat of the CIS in response to sea level or atmospheric warming probably occurred repeatedly during intervals of massive iceberg discharge in the North Atlantic for as long as the CIS maintained a marine margin. The vulnerability of the ice sheet relates to detachment of the marine margin of the Juan de Fuca Lobe, allowing the evacuation of the Juan de Fuca Strait and the subsequent beheading and northward calving of the Puget Lobe into deep marine water.

[22] **Acknowledgments.** I.L.H. thanks the National Science Foundation (NSF grant OCE-0425382 (Marine Geology and Geophysics)) for financial support. Samples were provided by T. F. Pedersen with the assistance of the Natural Sciences and Engineering Research Council of Canada. Additional assistance for radiocarbon analyses was provided T. Guilderson and the Institute of Geophysics and Planetary Physics, Lawrence Livermore National Laboratory (LLNL), University of California, and the Center for Accelerator Mass Spectrometry, LLNL. We thank the personnel of L. Wingate, K. Kimm, and E. Pettygrew for technical and laboratory assistance. We thank M. Sarnthein and W. Broecker for discussions and access to unpublished data and manuscripts. Finally, we would like to thank the shipboard party of the MD126/IMAGES VIII (MONA) cruise of the R/V *Marion Dufresne* operated by the French Polar Institute (IPEV).

References

Alley, R. B., S. Anandakrishnan, T. K. Dupont, B. R. Parizek, and D. Pollard (2007), Effect of sedimentation on ice-sheet grounding-line stability, *Science*, *315*, 1838–1841, doi:10.1126/science.1138396.

Anandakrishnan, S., G. A. Catania, R. B. Alley, and H. J. Horgan (2007), Discovery of till deposition at the grounding line of Whillans Ice Stream, *Science*, *315*, 1835–1838, doi:10.1126/science.1138393.

Atwater, B. (1986), Pleistocene glacial-lake deposits of the Sanpoil River valley, northeastern Washington, *U.S. Geol. Surv. Bull.*, 1661, 39 pp.

Bard, E., B. Hamelin, R. G. Fairbanks, and A. Zindler (1990), Calibration of the ^{14}C timescale over the past 30000 years using mass spectrometric U-Th ages from Barbados corals, *Nature*, *345*, 405–410, doi:10.1038/345405a0.

Bard, E., B. Hamelin, M. Arnold, L. Montaggioni, G. Cabioch, G. Faure, and F. Rougerie (1996), Deglacial sea-level record from Tahiti corals and the timing of global meltwater discharge, *Nature*, *382*, 241–244, doi:10.1038/382241a0.

Bard, E., M. Arnold, B. Hamelin, N. Tisnerat-Laborde, and G. Cabioch (1998), Radiocarbon calibration by means of mass spectrometric ^{230}Th/^{234}U and ^{14}C ages of corals: An updated database including samples from Barbados, *Mururoa and Tahiti, Radiocarbon*, *40*, 1085–1092.

Bischof, J. F., and D. A. Darby (1997), Mid- to Late Pleistocene ice drift in the western Arctic Ocean: Evidence for a different circulation in the past, *Science*, *277*, 74–78, doi:10.1126/science.277.5322.74.

Blaise, B., J. J. Clague, and R. W. Mathewes (1990), Time of maximum Late Wisconsin glaciation, west coast of Canada, *Quat. Res.*, *34*, 282–295, doi:10.1016/0033-5894(90)90041-I.

Booth, D. B., K. G. Troost, J. J. Clague, and R. B. Waitt (2004), The Cordilleran Ice Sheet, in *The Quaternary Period in the United States*, edited by A. R. Gillespie, S. C. Porter, and B. F. Atwater, chap. 2, pp.17–43, Elsevier, New York.

Broecker, W., and S. Barker (2007), A 190‰ drop in atmospheric Δ^{14}C during the "Mystery Interval" (17.5 to 14.5 kyr), *Earth Planet. Sci. Lett.*, *256*, 90–99, doi:10.1016/j.epsl.2007.01.015.

Clague, J. J., and T. S. James (2002), History and isostatic effects of the last ice sheet in southern British Columbia, *Quat. Sci. Rev.*, *21*, 71–87, doi:10.1016/S0277-3791(01)00070-1.

Clague, J. J., R. Barendregt, R. J. Enkin, and F. F. Foit (2003), Paleomagnetic and tephra evidence for tens of Missoula floods in southern Washington, *Geology*, *31*, 247–250, doi:10.1130/0091-7613(2003)031<0247:PATEFT>2.0.CO;2.

Clark, P. U., S. W. Hostetler, N. G. Pisias, A. Schmittner, and K. J. Meissner (2007), Mechanisms for a ~7-kyr climate and sea-level oscillation during marine isotope stage 3, in *Ocean Circulation: Mechanisms and Impacts*, *Geophys. Monogr. Ser.*, vol. 173, edited by A. Schmittner, J. Chiang, S. Hemmings, pp.198–209, AGU, Washington, D. C.

Clarke, G. K. C. (1987), Fast glacier flow: Ice streams, surging, and tidewater glaciers, *J. Geophys. Res.*, *92*, 8835–8841, doi:10.1029/JB092iB09p08835.

Cosma, T., I. L. Hendy, and A. Chang (2008), Chronological constraints on Cordilleran Ice Sheet glaciomarine sedimentation from MD02-2496 off Vancouver Island (western Canada), *Quat. Sci. Rev.*, doi:10.1016/j.quascirev.2008.01.013, in press.

Dethier, D. P., F. Pessl, R. F. Keuler, M. A. Balzarini, and D. R. Pevear (1995), Late Wisconsinan glaciomarine deposition and isostatic rebound, northern Puget lowland, Washington, *Geol. Soc. Am. Bull.*, *107*, 1288–1303, doi:10.1130/0016-7606(1995)107<1288:LWGDAI>2.3.CO;2.

Easterbrook, D. J. (1986), Stratigraphy and chronology of Quaternary deposits of the Puget lowland Olympic Mountains of Washington and the Cascade Mountains of Washington and Oregon, *Quat. Sci. Rev.*, *5*, 145–159, doi:10.1016/0277-3791(86)90180-0.

Fairbanks, R. G. (1989), A 17000-year glacio-eustatic sea level record: Influence of glacial melting rates on the Younger Dryas event and deep-ocean circulation, *Nature*, *342*, 637–642, doi:10.1038/342637a0.

Fairbanks, R. G., R. A. Mortlock, T. C. Chiu, L. Cao, A. Kaplan, T. P. Guilderson, T. W. Fairbanks, A. L. Bloom, P. M. Grootes, and M. J. Nadeau (2005), Radiocarbon calibration curve spanning 0 to 50000 years BP based on paired Th-^{230}Th/^{234}U/^{238}U and ^{14}C dates on pristine corals, *Quat. Sci. Rev.*, *24*, 1781–1796, doi:10.1016/j.quascirev.2005.04.007.

Grigg, L. D., and C. Whitlock (2002), Patterns and causes of millennial-scale climate change in the Pacific Northwest during marine isotope stages 2 and 3, *Quat. Sci. Rev.*, *21*, 2067–2083, doi:10.1016/S0277-3791(02)00017-3.

Guilbault, J. P., J. V. Barrie, K. Conway, M. Lapointe, and T. Radi (2003), Paleoenvironments of the Strait of Georgia, British Columbia during the last deglaciation: Microfaunal and microfloral evidence, *Quat. Sci. Rev.*, *22*, 839–857, doi:10.1016/S0277-3791(02)00252-4.

Haneburth, T., K. Stattegger, and P. M. Grootes (2000), Rapid Flooding of the Sunda Shelf: A late-glacial sea-level record, *Science*, *288*, 1033–1035.

Hemming, S. R. (2004), Heinrich events: Massive late Pleistocene detritus layers of the North Atlantic and their global climate imprint, *Rev. Geophys.*, *42*, RG1005, doi:10.1029/2003RG000128.

Hendy, I. L., J. P. Kennett, E. B. Roark, and B. L. Ingram (2002), Apparent synchroneity of submillennial scale climate events between Greenland and Santa Barbara Basin, California from 30–10 ka, *Quat. Sci. Rev.*, *21*, 1167–1184, doi:10.1016/S0277-3791 (01)00138-X.

Herzer, R. H., and B. D. Bornhold (1982), Glaciation and post-glacial history of the continental shelf off southwestern Vancouver Island, British Columbia, *Mar. Geol.*, *48*, 285–319, doi:10.1016/0025-3227(82)90101-3.

Hill, T. M., J. P. Kennett, D. K. Pak, R. J. Behl, C. Robert, and L. Beaufort (2006), Pre-Bølling warming in Santa Barbara Basin, California: Surface and intermediate water records of early deglacial warmth, *Quat. Sci. Rev.*, *25*, 2835–2845, doi:10.1016/j.quascirev.2006.03.012.

Hughen, K., S. Lehman, J. Southon, J. Overpeck, O. Marchal, C. Herring, and J. Turnbull (2004a), ^{14}C activity and global carbon cycle changes over the past 50000 years, *Science*, *303*, 202–207, doi:10.1126/science.1090300.

Hughen, K. A., et al. (2004b), Marine04 marine radiocarbon age calibration, 0–26 cal kyr BP, *Radiocarbon*, *46*, 1059–1086.

Hughen, K., J. Southon, S. Lehman, C. Bertrand, and J. Turnbull (2006), Marine-derived ^{14}C calibration and activity record for the past 50000 years updated from the Cariaco Basin, *Quat. Sci. Rev.*, *25*, 3216–3227, doi:10.1016/j.quascirev.2006.03.014.

Hutchinson, I., T. S. James, P. J. Reimer, B. D. Bornhold, and J. J. Clague (2004), Marine and limnic radiocarbon reservoir corrections for studies of late- and postglacial environments in Georgia Basin and Puget Lowland, British Columbia, Canada and Washington, USA, *Quat. Res.*, *61*, 193–203, doi:10.1016/j.yqres.2003.10.004.

Kitagawa, H., and J. vanderPlicht (1998), Atmospheric radiocarbon calibration to 45000 yr B. P.: Late glacial fluctuations and cosmogenic isotope production, *Science*, *279*, 1187–1190, doi:10.1126/science.279.5354.1187.

Kovanen, D. J., and D. J. Easterbrook (2002), Paleodeviations of radiocarbon marine reservoir values for the northeast Pacific, *Geology*, *30*, 243–246, doi:10.1130/0091-7613(2002)030<0243:PORMRV>2.0.CO;2.

Marchitto, T. M., S. J. Lehman, J. D. Ortiz, J. Fluckiger, and A. van Geen (2007), Marine radiocarbon evidence for the mechanism of deglacial atmospheric CO_2 rise, *Science*, *316*, 1456–1459, doi:10.1126/science.1138679.

McKay, J. L., T. F. Pedersen, and S. S. Kienast (2004), Organic carbon accumulation over the last 16 kyr off Vancouver Island, Canada: Evidence for increased marine productivity during the deglacial, *Quat. Sci. Rev.*, *23*, 261–281, doi:10.1016/j.quascirev.2003.07.004.

McKay, J. L., T. F. Pedersen, and J. Southon (2005), Intensification of the oxygen minimum zone in the northeast Pacific off Vancouver Island during the last deglaciation: Ventilation and/or export production?, *Paleoceanography*, *20*, PA4002, doi:10.1029/2003PA000979.

McManus, J. F., R. Francois, J. M. Gherardi, L. D. Keigwin, and S. Brown-Leger (2004), Collapse and rapid resumption of Atlantic meridional circulation linked to deglacial climate changes, *Nature*, *428*, 834–837, doi:10.1038/nature02494.

Meier, M. F., and A. Post (1987), Fast tidewater glaciers, *J. Geophys. Res.*, *92*, 9051–9058, doi:10.1029/JB092iB09p09051.

Minobe, S., and N. Mantua (1999), Interdecadal modulation of interannual atmospheric and oceanic variability over the North Pacific, *Prog. Oceanogr.*, *43*, 163–192, doi:10.1016/S0079-6611(99)00008-7.

Mosher, D. C., and A. T. Hewitt (2004), Late Quaternary deglaciation and sea-level history of eastern Juan de Fuca Strait, Cascadia, *Quat. Int.*, *121*, 23–39, doi:10.1016/j.quaint.2004.01.021.

Porter, S. C., and T. W. Swanson (1998), Radiocarbon age constraints on rates of advance and retreat of the Puget lobe of the Cordilleran ice sheet during the last glaciation, *Quat. Res.*, *50*, 205–213, doi:10.1006/qres.1998.2004.

Rea, D. K., and T. R. Janecek (1981), Mass-accumulation rates of the non-authigenic organic crystalline (Eolian) component of deep-sea sediments from the western mid-Pacific mountains, *Deep Sea Drilling Site 463, Proc. Ocean Drill. Program Initial Rep.*, edited by J. Thiede and T. L. Vallier, *62*, 653–659.

Rohling, E. J., R. Marsh, N. C. Wells, M. Siddall, and N. R. Edwards (2004), Similar meltwater contributions to glacial sea level changes from Antarctic and northern ice sheets, *Nature*, *430*, 1016–1021, doi:10.1038/nature02859.

Sarnthein, M., T. Kiefer, P. M. Grootes, H. Elderfield, and H. Erlenkeuser (2006), Warmings in the far northwestern Pacific promoted pre-Clovis immigration to America during Heinrich event 1, *Geology*, *34*, 141–144, doi:10.1130/G22200.1.

Sarnthein, M., P. Grootes, J. P. Kennett, and M. J. Nadeau (2007), ^{14}C reservoir ages show deglacial changes in ocean currents and carbon cycle, in *Ocean Circulation: Mechanisms and Impacts*, *Geophys. Monogr. Ser.*, vol. 173, edited by A. Schmittner, J. Chiang, and S. Hemmings, pp. 175–196, AGU, Washington, D. C.

Siddall, M., E. J. Rohling, A. Almogi-Labin, C. Hemleben, D. Meischner, I. Schmelzer, and D. A. Smeed (2003), Sea-level fluctuations during the last glacial cycle, *Nature*, *423*, 853–858, doi:10.1038/nature01690.

St. John, K. E. K., and L. A. Krissek (1999), Regional patterns of Pleistocene ice-rafted debris flux in the North Pacific, *Paleoceanography*, *14*, 653–662, doi:10.1029/1999PA900030.

Stuiver, M., and P. M. Grootes (2000), GISP2 oxygen isotope ratios, *Quat. Res.*, *53*, 277–283, doi:10.1006/qres.2000.2127.

Stuiver, M., P. M. Grootes, and T. F. Braziunas (1995), The GISP2 $\delta^{18}O$ climate record of the past 16,500 years and the role of the Sun, ocean, and volcanoes, *Quat. Res.*, *44*, 341–354, doi:10.1006/qres.1995.1079.

Telford, R. J., E. Heegaard, and H. J. B. Birks (2004), The intercept is a poor estimate of a calibrated radiocarbon age, *Holocene*, *14*, 296–298, doi:10.1191/0959683604hl707fa.

Thorson, R. M. (1980), Ice-sheet glaciation of the Puget Lowland, Washington, during the Vashon Stade (late Pleistocene), *Quat. Res.*, *13*, 303–321, doi:10.1016/0033-5894(80)90059-9.

van der Plicht, J., et al. (2004), NotCal04; comparison/calibration ^{14}C records 26–50 cal kyr BP, *Radiocarbon*, *46*, 1225–1238.

vanKreveld, S., M. Sarnthein, H. Erlenkeuser, P. Grootes, S. Jung, M. J. Nadeau, U. Pflaumann, and A. Voelker (2000), Potential links between surging ice sheets, circulation changes, and the Dansgaard-Oeschger cycles in the Irminger Sea, 60–18 kyr, *Paleoceanography*, *15*, 425–442, doi:10.1029/1999PA000464.

Voelker, A. H. L., M. Sarnthein, P. M. Grootes, H. Erlenkeuser, C. Laj, A. Mazaud, M. J. Nadeau, and M. Schleicher (1998), Correlation of marine ^{14}C ages from the Nordic Seas with the GISP2 isotope record: Implications for ^{14}C calibration beyond 25 ka BP, *Radiocarbon*, *40*, 517–534.

Waitt, R., and R. Thorson (1983), The Cordilleran Ice Sheet in Washington, in *Late-Quaternary Environments of the United States*, edited by H. E. Wright and S. C. Porter, pp. 53–70, Univ. of Minn. Press, Minneapolis.

Wang, Y. J., H. Cheng, R. L. Edwards, Z. S. An, J. Y. Wu, C. C. Shen, and J. A. Dorale (2001), A high-resolution absolute-dated Late Pleistocene monsoon record from Hulu Cave, *China, Science*, *294*, 2345–2348, doi:10.1126/science.1064618.

T. Cosma and I. L. Hendy, Department of Geological Sciences, University of Michigan, 1100 North University Avenue, Ann Arbor, MI 48109-1005, USA. (ihendy@umich.edu)